HHS Public Access

Author manuscript

Biomaterials. Author manuscript; available in PMC 2016 September 01.

Published in final edited form as:

Biomaterials. 2015 September ; 62: 88–94. doi:10.1016/j.biomaterials.2015.05.009.

Pediatric Tubular Pulmonary Heart Valve from Decellularized Engineered Tissue Tubes

Jay M. Reimer[1], **Zeeshan H. Syedain**[1], **Bee H.T. Haynie**, and **Robert T. Tranquillo**[1,2]

[1]Department of Biomedical Engineering, University of Minnesota

[2]Department of Chemical Engineering and Material Science, University of Minnesota

Abstract

Pediatric patients account for a small portion of the heart valve replacements performed, but a pediatric pulmonary valve replacement with growth potential remains an unmet clinical need. Herein we report the first tubular heart valve made from two decellularized, engineered tissue tubes attached with absorbable sutures, which can meet this need, in principle. Engineered tissue tubes were fabricated by allowing ovine dermal fibroblasts to replace a sacrificial fibrin gel with an aligned, cell-produced collagenous matrix, which was subsequently decellularized. Previously, these engineered tubes became extensively recellularized following implantation into the sheep femoral artery. Thus, a tubular valve made from these tubes may be amenable to recellularization and, ideally, somatic growth.

The suture line pattern generated three equi-spaced “leaflets” in the inner tube, which collapsed inward when exposed to back pressure, per tubular valve design. Valve testing was performed in a pulse duplicator system equipped with a secondary flow loop to allow for root distention. All tissue-engineered valves exhibited full leaflet opening and closing, minimal regurgitation (< 5%), and low systolic pressure gradients (< 2.5 mmHg) under pulmonary conditions. Valve performance was maintained under various trans-root pressure gradients and no tissue damage was evident after 2 million cycles of fatigue testing.

Keywords

Tubular Heart Valve; Fibrin; Cardiac Tissue Engineering; Pulse Duplicator; Decellularization

1.0 Introduction

Valvular heart disease affects ~2.5% of the U.S. population and there were more than 110,000 heart valve procedures in 2011 [1,2]. There is a clinical need for a new prosthetic pulmonary valve (PV) despite the fact that this valve accounted for only ~1.3% of all heart

corresponding author: Robert T. Tranquillo, Department of Biomedical Engineering, 312 Church St SE, University of Minnesota, Minneapolis, MN 55455, Tel: 612-625-6868, Fax: 612-626-6583, tranquil@umn.edu.

valve procedures in the U.S. in 2011 [1]. Current PV prostheses are not ideal for “pediatric patients” (younger than 18 years old) due to their inability to grow. Current commercially-available PV prostheses include homograft valves (cryo-preserved or decellularized) and a chemically-fixed bovine jugular vein graft (trileaflet) [3,4]. Glutaraldehyde-fixation eliminates the immunogenicity of xenogeneic tissue, but also limits cell invasion and ultimately somatic growth [5]. Thus, young patients typically undergo multiple operative procedures in order to replace outgrown PV prostheses during maturation.

Numerous tissue-engineered heart valves (TEHVs) have been explored in hopes of developing “living” valves capable of *in vivo* tissue remodeling and growth [6-11]. Various strategies have been used for tissue fabrication, including the use of cell-seeded hydrogels with or without a polymeric co-scaffold. Although initially functional, many of these TEHVs exhibited progressive leaflet retraction during preclinical animal studies [10,12]. This has been attributed to sustained contraction of the transplanted cells, leading researchers to decellularize the tissue prior to implantation [13-15]. Although somatic growth has not yet been demonstrated, there have been several reports of decellularized tissue being recellularized [16,17], which is a necessary precursor to tissue remodeling and growth.

Earlier valve iterations focused on mimicking the shape of natural valve leaflets and often utilized complex molds [7,18,19]. More recently, TEHVs with a tubular leaflet design have been explored that do not rely on complex molds. To date, these tubular TEHVs have all used a single tube – attached to a stent, frame, or within an inert conduit – to generate a valve-like action [13,15,20]. Our group has previously reported a tubular TEHV using a single tube, generated by entrapping fibroblasts in a sacrificial fibrin gel, onto a PEEK frame [21]. Despite the promising functional performance of this TEHV, its inert frame precludes it from growing and thus renders it suboptimal for pediatric PV replacements.

In this study we report a frameless, tubular TEHV generated from two decellularized engineered tissue tubes (referred to as “engineered tubes” hereafter) sewn together in a specified pattern using degradable sutures. The outer tube serves as the flow conduit and provides the mechanical constraints needed for the inner tube to function as “leaflets”, as in classic tubular valve design. The regions of the inner tube not mechanically constrained by the outer tube collapse inward when exposed to back pressure. The engineered tubes were fabricated by entrapping ovine dermal fibroblasts in a tubular fibrin gel, as previously discussed [13]. The entrapped cells replaced the fibrin with a collagenous matrix, which is anisotropic due to the mechanical constraints imposed during the culture period. Collagen production was stimulated by stretching the constructs in a pulsed flow-stretch bioreactor following an initial static culture period. Decellularization in sequential detergent treatments was then used to remove the cellular components.

Following engineered tube and valve fabrication, the TEHVs were functionally tested in a custom pulse duplicator system to assess valve performance and root distention under pulmonary conditions. The durability of the suture line was assessed by fatiguing one TEHV for two weeks. Macroscopic appearance and valve performance metrics were compared before, during, and after fatiguing to assess the TEHV’s durability. Valve performance and

mechanical properties were compared to those from a commercially-available, pulmonary valve prosthesis (Medtronic Contegra valve).

2.0 Materials and Methods

2.1 Tissue Fabrication

A cell-entrapped, isotropic fibrin gel was formed by mixing bovine fibrinogen (Sigma), ovine dermal fibroblasts (Coriell), thrombin (Sigma), and calcium chloride. Final component concentrations of the gel were as follows: 4 mg/mL fibrinogen, 1 million cells/mL, 0.38 U/mL thrombin, and 5 mM $CaCl_2$. This solution was injected into a tubular mold, formed by inserting a 19 mm glass rod into a concentric, polycarbonate tube (Figure 1a). The glass rods were pre-fitted with Dacron© cuffs on either end to aid in handling and pretreated with 5% Pluronic F-127 (Sigma) in double-distilled water.

Following gelation, the glass molds were removed from the polycarbonate outer casings and cultured in DMEM supplemented with 10% fetal bovine serum (FBS, HyClone), 100 U/mL penicillin, 100 μg/mL streptomycin, 0.25 μg/mL amphotericin B, 2 μg/mL insulin, and 50 μg/mL ascorbic acid. After two weeks, the tissue tubes were transferred onto 16 mm latex tubes, attached to custom manifolds, and cyclically stretched in a pulsed-flow-stretch bioreactor for 5 weeks [22]. Construct stretching began at 3% strain and was increased weekly by 1% until a 5% maximum strain was achieved.

2.1.1 Tissue Tube Decellularization—The tissue tubes were treated with 1% sodium dodecyl sulfate (SDS, Sigma) in distilled water for 6 hours (replaced after 1, 3, and 5 hours) at room temperature with continuous shaking. Following SDS treatment, the tubes underwent 3 × 10 minute washes in 1% Triton X-100 (Sigma) in distilled water at room temperature. The tubes were extensively rinsed in phosphate buffered saline (PBS) for one week at 4° Celsius before and after overnight incubation in DMEM supplemented with 10% FBS and 2 U/mL deoxyribonuclease (Worthington Biochemical).

2.2 Valve Fabrication

Four TEHVs were fabricated, each of which used two 16 mm inner diameter engineered tubes, which were trimmed to an axial length of either ~15 mm or ~12 mm. The tubes were sewn together, with the shorter tube inside of the longer tube, using absorbable 7-0 Maxon CV (Covidien) sutures. The pattern of the first suture line (Figure 2a, green dashed line) defined commissure and “leaflet” regions. Independent, crosshatched suture lines were then added to reinforce each commissure (Figure 2a, purple dashed line) on the three subsequent TEHVs.

2.3 Pulse Duplicator Testing

Four TEHVs and one commercial pediatric pulmonary valve (Medtronic Contegra, 18 mm ID) were tested in a custom pulse duplicator system. One TEHV (no cross-hatching pattern) was used to assess root strain at different trans-root pressure gradients. These pressure gradients were prescribed by adjusting the ablumenal pressure on the TEHV, while maintaining the lumenal pressure and waveforms (by keeping the pump displacement

constant). One TEHV was fatigued at pulmonary pressure conditions for two weeks real-time at 100 cycles/minute and was functionally characterized (with a higher flowrate) before, after 1 week, and at the conclusion of the fatiguing regimen. Two other TEHVs and the Contegra valve were functionally characterized, but not fatigued.

The pulse duplicator system consisted of a pulse generator, compliance chambers, and two flow loops (Figure 3a). The pulse generator pumped fluid through an electromagnetic flowmeter (Carolina Medical) and test valve before being returned to the reservoir in the primary flow loop, as previously described [21]. Unidirectional flow was ensured by placing a bileaflet, mechanical valve downstream of the reservoir. For these tests, a secondary flow loop was added that exited from the top of the fluid-filled chamber where the test valve was mounted (Figure 3a). A downstream needle valve controlled the trans-root flow and was used to regulate the pressure on the ablumenal surface of the test valve. System compliance, for both flow loops, was modulated by changing the fluid level in air-filled chambers upstream and downstream of the test valve.

Transducers (Vivitro Systems) were placed downstream, upstream, and on the ablumenal surface of the test valve to record system pressures. Instantaneous flowrates were measured using an electromagnetic flowmeter (Carolina Medical) placed between the pulse generator and test valve. Flowrates and system pressures were recorded using a custom LabVIEW program and analyzed using a custom Matlab script (see Figure 3b for a representative waveform). All pressure and flow metrics reported in Tables 2 & 3 were averaged over 3 cycles for each valve. Diastolic pressure drop was defined as the average difference between the inflow and outflow pressures over the period of the cycle when the flowrate was less than or equal to zero. Systolic pressure drop was defined as the average pressure difference over the period of the cycle when the inflow pressure exceeded the outflow pressure. Mean forward flowrate is the average of the forward flow portion of the flow trace. Regurgitation refers to ratio of total negative flow to the stroke volume, or positive flow, for each cycle. Additional information on these metrics can be found in ISO 5840.

There was a “water hammer” effect during valve closure that resulted in a substantial pressure spike on the inflow side of the valve, though it is noticeable in all three pressure traces (Figure 3b). This pressure spike was noticeably larger in one of the TEHVs, which resulted in a higher diastolic pressure drop at the desired mean forward flowrate. The magnitude of the spike was reduced by increasing the ventricular compliance of the system. However, this resulted in a second positive flow pulse after the TEHV closed. Therefore, only the regions before this secondary pulse were used to calculate the mean diastolic pressure drop and regurgitation for this TEHV.

Lumenal and ablumenal videos of the test valve were recorded during testing at 50 fps (Canon Rebel T3i) and analyzed in ImageJ to assess geometric orifice area (GOA) and maximum root strain. GOA is defined as the ratio of the open area during systole to the maximum cross-sectional area of the valve leaflets. For this study, the maximum (viewable) cross-sectional area is dependent on the inner diameter of the silicone tubes (16 mm), which are attached to each end of the test valve and prevent paravalvular leak. Maximum root

strain was taken as the natural logarithm of the maximum over the minimum root diameter, as determined in ImageJ.

2.4 Macroscopic Tissue Imaging & Histology

Valves were macroscopically visualized using a stereoscope (Leica StereoZoom 4) outfitted with a digital camera (Canon Rebel T3i). Images of the suture lines, as seen from the ablumenal and lumenal surfaces, were captured before, during, and after valve testing. For histology, tissue strips were cut and fixed in 4% paraformaldehyde at 4° Celsius and frozen in OCT (Tissue-Tek) using liquid nitrogen. 9 μm cross-sections were sliced and stained with Lillie's trichrome and picrosirius red. Images were taken using a color CCD camera from an Olympus IX70 microscope at 4X magnification. For picrosirius red staining, the samples were placed between crossed plane polarizers during imaging.

2.5 Tensile Mechanical Testing

Strips, parallel ("circumferential") and orthogonal ("radial") to the circumference of the tubes, were cut (~2 mm × 12 mm) from the engineered tubes and mechanically characterized. Strips from the Contegra valve's leaflets and root were also characterized. The engineered tubes used for the TEHV were fundamentally the same, so separate "root" and "leaflet" mechanical properties were not reported. Sample dimensions were measured prior to testing using a digital caliper.

The strips were mounted in custom grips attached to the tester's actuator arms and straightened with a 0.005 N tensile load. Six preconditioning cycles were performed (0-10% strain) before the samples were strained to failure at 3 mm/min using an Instron MicroBionix (Instron Systems). Strain was calculated by taking the natural logarithm of the sample's deformed length over its initial length. Stress was defined as the force divided by the undeformed, cross-sectional area of the strip. Modulus and ultimate tensile strength (UTS) were taken as the slope of the linear region of the stress-strain curve and the maximum stress recorded, respectively.

2.6 Suture Retention Testing

The suture tension properties were also evaluated for the engineered tubes, in accordance with ISO 7198. Briefly, a 6-0 prolene suture was passed through the circumferential strips (~5 mm × 10 mm) 2 mm from the free edge. The suture was tied into a loop and then pulled at a rate of 50 mm/min axially, or orthogonal to the presumed fiber direction, through the strips using the Instron MicroBionix tester.

3.0 Results

3.1 Tissue Fabrication and Characterization

Engineered tissue tubes were fabricated by allowing entrapping ovine dermal fibroblast in a cylindrical fibrin gel (Figure 1a). The entrapped cells replaced the fibrin (Figure 1b, red stain) with circumferentially-aligned, cell-produced collagen (Figure 1b, green stain). Decellularization removed cell components, leaving a matrix-only engineered tube, as shown in Figure 1b. Collagen fibers were visualized by staining with picrosirius red and

imaged under crossed plane polarizers (Figure 1c). The intensity of red is directly related to collagen packing and alignment [23].

The engineered tubes were tested for their tensile mechanical properties and compared to those for the Contegra valve, a commercial pediatric pulmonary valve (Table 1). The engineered tubes exhibited anisotropy, which is characteristic of native cardiovascular tissues. The thickness of the Contegra valve's leaflets (0.21 ± .03 mm) and root (0.76 ± 0.10 mm) were different than the thickness of the engineered tubes (1.35 ± 0.05 mm). The suture retention strength of the engineered tissue was 175 ± 54 grams force.

3.2 Tubular TEHV Fabrication and Characterization

TEHVs were fabricated by sewing 2 concentric, engineered tubes together using absorbable sutures in a prescribed pattern (Figure 2a). The geometry of the sewing pattern dictated the behavior of the inner tube when exposed to forward and reverse flow. The tubes were attached around their entire circumference by the first sewing pattern (purple line in Figure 2a). The three commissure regions (one is shown in Figure 2b) mechanically constrained the inner tube from collapsing near its free edge, analogous to the posts on a framed valve. The three commissure regions were reinforced with a second sewing pattern (green line in Figure 2a) to increase the number of anchor points. The three "leaflets", or regions between adjacent commissures on the inner tube, were not mechanically constrained at their free edge and collapsed inward to close the TEHV when exposed to back pressure (Figure 2c). The outer tube functioned as the flow conduit of the valve and provided structural support for the inner tube (Figure 2a).

3.3 In Vitro Performance Testing

Three TEHVs and a control valve (Contegra valve) were tested in a pulse duplicator system (Figure 3a) at pulmonary conditions with a mean forward flowrate of 3.6 ± 0.2 L/min. A representative pressure and flow waveform is shown in Figure 3b and their line colors correspond with the pressure and flow sensors shown in Figure 3a. Each of the TEHVs tested had lower regurgitation and mean systolic pressure drop compared to the Contegra valve, as seen in Table 2. Additionally, the GOA for the Contegra valve (52%) was substantially lower than for the TEHVs (76% ± 15%) despite the Contegra valve's leaflets being much thinner. Representative still frames of the TEHV opening are shown in Figure 4. The TEHV fully closed (Figure 4a) during diastole and then began to symmetrically open (Figure 4b-d) before achieving maximum opening (Figure 4e) at peak systole.

3.4 Trans-Root Pressure Manipulation

TEHV root distention and valve function were assessed under various trans-root pressure gradients, ranging from 27.2 to 39.1 mmHg (Figure 5). Mean diastolic pressure drop and mean forward flowrate were ~15 mmHg and ~1.7 L/min for all cases, respectively. Maximum circumferential root strain ranged from 0.8% to 2.7% and was linearly dependent on the trans-root pressure gradient (Figure 5a). TEHV regurgitation and maximum GOA were maintained independent of trans-root pressure gradients (values remained within 4% of each other for all of the test cases reported) as shown in Figure 5b and 5c, respectively.

These valve performance metrics were normalized by their respective values at maximum root distention (2.7%).

3.5 TEHV Fatiguing

One TEHV was fatigued in the pulse duplicator system for 2 weeks at 100 cycles/minute and a mean diastolic pressure drop of 7.4 – 8.7 mmHg. The mean forward flowrate was only ~1.9 L/min, but the testing conformed to ISO 5840 in that the valve was able to fully open and close during each cycle. The entire TEHV was visually inspected using a stereoscope, but particular attention was given to the commissure regions as seen from the ablumenal and lumenal surfaces (Figure 6a). Macroscopic tissue damage was not detected before (Figure 6b-c), during (Figure 6d-e), or after (Figure 6f-g) fatiguing. It did appear that the suture lines, particularly the cross-hatched pattern, became looser over the course of fatiguing (Figure 6b, d, and f). However, the inner tube remained firmly attached to the outer tube (Figure 6c, e, and g).

TEHV GOA increased from 81% before fatiguing to 89% and 87% after 1 and 2 weeks, respectively (Table 3). One leaflet of the TEHV developed a slight prolapse during diastole after the first week of fatiguing. This development was represented by the increase in regurgitation from 3.9% to 12.9% (Table 3). However, the prolapse and regurgitation did not progress over the final week of fatiguing and did not lead to any observable tissue damage on the suture line.

4.0 Discussion

We have previously developed a TEHV using a single engineered tube attached to a frame [21]. This valve had characteristic anisotropic leaflet stiffness and performance at physiological conditions with a small systolic pressure drop and trivial regurgitation. However, the engineered tube was mounted onto a non-degradable frame, which made it suboptimal for pediatric patients since it precludes somatic growth. In this iteration of our TEHV, we have developed a frameless valve that is more suitable for pediatric patients since it has the potential to grow and remodel. It consists of two engineered tubes that were sewn together using degradable sutures. Since the sutures will completely degrade, host cell invasion will be critical to the TEHV's *in vivo* growth and remodeling potential.

Previous attempts at developing a valve from a single mold, with fibrin as the scaffold, have been reported by our group and others [7,11,18]. While these valve designs provided a proof of concept, there are several challenges associated with the single mold approach. One major challenge is creating leaflets with the appropriate initial thickness while ensuring that coaptation and mechanical strength are maintained as the fibrin gel is contracted by the entrapped cells. Further challenges included machining complex molds and high stress on sharp corners of the mold, leading to thinning and tearing in the engineered tissue.

While tubular valve design addresses many of the challenges associated with the single mold design, it relies on the two engineered tubes fusing during *in vivo* remodeling. The sutures in the proposed design were selected based on their slow degradation rate, which will allow them to provide mechanical support during *in vivo* recellularization and tissue remodeling.

In previous studies by our group using similarly decellularized tissue implanted as arterial grafts, we showed recellularization spanning the entire length (2-3 cm) of the graft after 8 weeks [24,25]. If the valve leaflets have similar host cell invasion and matrix deposition, then the timing of suture degradation and recellularization would match fairly well.

Demonstrating somatic growth by replacing the pulmonary artery using a vascular graft made from degradable polymers has been tested in a lamb model. In the study by Hoerstrup *et al.*, a degradable polymer graft was seeded with autologous cells from a lamb and evaluated for growth and remodeling [26]. The graft was harvested after 100 weeks and it showed progressive growth, complete degradation of the synthetic polymer, and host tissue replacing the entire structure of the graft. Another study reported remodeling and an increase in size of a synthetic polymer graft seeded with bone marrow mononuclear cells over 6 months implanted into the inferior vena cava of a lamb [27].

Based on these two studies and our previous arterial graft study [24,25], we expect our tissue to be amenable to host cell invasion. To ensure that our proposed valve design is capable of withstanding the initial phase of cellular ingrowth and suture degradation, we performed several *in vitro* tests to assess its durability. The most relevant test was to fatigue the TEHV at pulmonary pressure conditions (i.e. physiologic end-diastolic pressure drop with complete valve opening and closing). This testing was performed for more than 2 million cycles and there was no noticeable change in the sutures, tearing, or tissue damage. However, one leaflet developed a slight prolapse, possibly due to asymmetry in the “leaflets” as sewn or prolonged exposure to the water-hammer effect, which led to increased regurgitation after 1 week. While longer testing could have been performed, we consider this number of cycles to be sufficient to assess the TEHV’s current design. Important questions regarding the TEHV’s growth, remodeling, and tissue fusion cannot be answered with *in vitro* fatigue testing.

While this is the first tubular valve design using two completely-biological engineered tubes, other groups have explored tissue-engineered valves with various designs. One design from Weber *et al*. embedded a knitted, non-degradable, synthetic polymer tube within a cell-containing fibrin gel in a tubular geometry [15,20]. These proof of concept studies were done by connecting the fibrin/polymer mesh to a silicone outer tube or nitinol stent to generate “leaflets”. The advantage of this approach is that the initial strength of the synthetic polymer provides a durable anchor for attachment, while still providing a biological matrix for cellular remodeling. However, mechanical anisotropy similar to native leaflets was a critical design criterion in our approach and the inclusion of any polymer mesh would preclude fibrin gel compaction and associated mechanical anisotropy. The suture retention strength of our engineered tissue allowed us to sew the tubes together without synthetic polymer reinforcement. Compliance mismatch in a composite structure could also have detrimental effects during fatigue testing or during *in vivo* testing, which was not reported. Moreover, their design using a non-degradable, synthetic polymer tube or inert stent would not be suitable for pediatric applications.

Functionally, we evaluated the tissue-engineered valve in a pulse duplicator and compared the values to a commercial pediatric pulmonary valve (Contegra 18 mm diameter conduit,

Medtronic). One of the critical parameters for a pulmonary valve replacement is its systolic pressure drop. While the engineered (ovine) tissue used in this study was much thicker than the Contegra valve's leaflets, the systolic pressure drop of the TEHV was lower than the Contegra's under similar testing conditions. This was potentially due to the non-fixed, compliant nature of the engineered matrix. Regurgitation (including closing volume) is another critical parameter and was also lower in our TEHV compared to the Contegra valve.

We also evaluated the effects of variable trans-root pressure gradients to ensure that valve coaptation, maximum valve opening, and regurgitation were not adversely affected. This is relevant because certain congenital defects can lead to pulmonary artery hypertension, which is defined as when the mean pulmonary pressure exceeds 25 mmHg *in vivo* [28,29]. Theoretical outer diameters were calculated (data not shown) using the Law of Laplace for thick-walled right cylinders [30], but did not fully agree with the measured values. Several aspects of the test system could account for these differences, such as the "wall" being non-continuous due to the presence of separate inner and outer tubes. Additionally, the relatively small axial length to diameter aspect ratio of the TEHV and the presence of suture lines could account for some of the differences observed.

Overall, the pulse duplicator testing and fatigue testing provide strong evidence that the current valve design will exhibit excellent initial performance in the pulmonary position. Whether the valve remodels to same extent as seen previously in arterial position remains to be seen and will be the focus of a subsequent *in vivo* study.

Acknowledgement

Authors acknowledge technical assistance from Naomi Ferguson, Sandy Johnson, Susan Saunders, and Jill Schmidt and funding from NIH R01 HL107572 to R.T.T.

References

[1]. Quality AfHRa. Healthcare cost and utilization project (hcup). 2014. http://hcupnet.ahrq.gov/

[2]. Lloyd-Jones D, Adams RJ, Brown TM, Carnethon M, Dai S, De Simone G, et al. Heart disease and stroke statistics--2010 update: A report from the american heart association. Circulation. 2010; 121(7):e46–e215. [PubMed: 20019324]

[3]. Protopapas AD, Athanasiou T. Contegra conduit for reconstruction of the right ventricular outflow tract: A review of published early and mid-time results. J Cardiothorac Surg. 2008; 3:62. [PubMed: 19017382]

[4]. Ruzmetov M, Shah JJ, Geiss DM, Fortuna RS. Decellularized versus standard cryopreserved valve allografts for right ventricular outflow tract reconstruction: A single-institution comparison. J Thorac Cardiovasc Surg. 2012; 143(3):543–9. [PubMed: 22340029]

[5]. Gulbins H, Goldemund A, Anderson I, Haas U, Uhlig A, Meiser B, et al. Preseeding with autologous fibroblasts improves endothelialization of glutaraldehyde-fixed porcine aortic valves. J Thorac Cardiovasc Surg. 2003; 125(3):592–601. [PubMed: 12658201]

[6]. Syedain ZH, Tranquillo RT. Controlled cyclic stretch bioreactor for tissue-engineered heart valves. Biomaterials. 2009; 30(25):4078–84. [PubMed: 19473698]

[7]. Flanagan T, Cornelissen C, Koch S, Tschoeke B, Sachweh J, Schmitz-Rode T, et al. The in vitro development of autologous fibrin-based tissue-engineered heart valves through optimized dynamic conditioning. Biomaterials. 2007; 28:3388–97. [PubMed: 17467792]

[8]. Gottlieb D, Kunal T, Emani S, Aikawa E, Brown DW, Powell AJ, et al. In vivo monitoring of function of autologous engineered pulmonary valve. J Thorac Cardiovasc Surg. 2010; 139(3): 723–31. [PubMed: 20176213]

[9]. Ramaswamy S, Gottlieb D, Engelmayr GC, Aikawa E, Schmidt DE, Gaitan-Leon DM, et al. The role of organ level conditioning on the promotion of engineered heart valve tissue development in-vitro using mesenchymal stem cells. Biomaterials. 2010; 31(6):1114–25. [PubMed: 19944458]

[10]. Flanagan TC, Sachweh JS, Frese J, Schnoring H, Gronloh N, Koch S, et al. In vivo remodeling and structural characterization of fibrin-based tissue-engineered heart valves in the adult sheep model. Tissue Eng Part A. 2009; 15(10):2965–76. [PubMed: 19320544]

[11]. Mol A, Driessen NJ, Rutten MC, Hoerstrup SP, Bouten CV, Baaijens FP. Tissue engineering of human heart valve leaflets: A novel bioreactor for a strain-based conditioning approach. Ann Biomed Eng. 2005; 33(12):1778–88. [PubMed: 16389526]

[12]. Syedain ZH, Lahti MT, Johnson SL, Ruth GR, Bianco R, Tranquillo RT. Implantation of a tissue-engineered heart valve from human fibroblasts exhibiting short term function in the sheep pulmonary artery. Cardiovasc Eng Technol. 2011; 2(2):101–12.

[13]. Syedain ZH, Meier LA, Reimer JM, Tranquillo RT. Tubular heart valves from decellularized engineered tissue. Ann Biomed Eng. 2013; 41(12):2645–54. [PubMed: 23897047]

[14]. Driessen-Mol A, Emmert MY, Dijkman PE, Frese L, Sanders B, Weber B, et al. Transcatheter implantation of homologous “off-the-shelf” tissue-engineered heart valves with self-repair capacity: Long-term functionality and rapid in vivo remodeling in sheep. J Am Coll Cardiol. 2014; 63(13):1320–9. [PubMed: 24361320]

[15]. Weber M, Heta E, Moreira R, Gesche VN, Schermer T, Frese J, et al. Tissue-engineered fibrin-based heart valve with a tubular leaflet design. Tissue Eng Part C Methods. 2014; 20(4):265–75. [PubMed: 23829551]

[16]. Driessen-Mol A, Dijkman PE, Frese L, Emmert MY, Grunenfelder J, Sidler M, et al. Decellularized in-vitro tissue-engineered heart valves - first in-vivo results. Biomaterials. 2012; 2012(4)

[17]. Weber B, Dijkman PE, Scherman J, Sanders B, Emmert MY, Grunenfelder J, et al. Off-the-shelf human decellularized tissue-engineered heart valves in a non-human primate model. Biomaterials. 2013; 34(30):7269–80. [PubMed: 23810254]

[18]. Robinson PS, Johnson SL, Evans MC, Barocas VH, Tranquillo RT. Functional tissue-engineered valves from cell-remodeled fibrin with commissural alignment of cell-produced collagen. Tissue Eng Part A. 2008; 14(1):83–95. [PubMed: 18333807]

[19]. Jockenhoevel S, Chalabi K, Sachweh JS, Groesdonk HV, Demircan L, Grossmann M, et al. Tissue engineering: Complete autologous valve conduit--a new moulding technique. Thorac Cardiovasc Surg. 2001; 49(5):287–90. [PubMed: 11605139]

[20]. Moreira R, Velz T, Alves N, Gesche VN, Malischewski A, Schmitz-Rode T, et al. Tissue-engineered heart valve with a tubular leaflet design for minimally invasive transcatheter implantation. Tissue Eng Part C Methods. 2014

[21]. Syedain ZH, Bradee AR, Kren S, Taylor DA, Tranquillo RT. Decellularized tissue-engineered heart valve leaflets with recellularization potential. Tissue Eng Part A. 2013; 19(5-6):759–69. [PubMed: 23088577]

[22]. Syedain ZH, Meier LA, Bjork JW, Lee A, Tranquillo RT. Implantable arterial grafts from human fibroblasts and fibrin using a multi-graft pulsed flow-stretch bioreactor with noninvasive strength monitoring. Biomaterials. 2011; 32(3):714–22. [PubMed: 20934214]

[23]. Dayan D, Hiss Y, Hirshberg A, Bubis JJ, Wolman M. Are the polarization colors of picrosirius red-stained collagen determined only by the diameter of the fibers? Histochemistry. 1989; 93(1): 27–9. [PubMed: 2482274]

[24]. Syedain ZH, Meier LA, Lahti MT, Johnson SL, Tranquillo RT. Implantation of completely biological engineered grafts following decellularization into the sheep femoral artery. Tissue Eng Part A. 2014; 20(11-12):1726–34. [PubMed: 24417686]

[25]. Meier LA, Syedain ZH, Lahti MT, Johnson SS, Chen MH, Hebbel RP, et al. Blood outgrowth endothelial cells alter remodeling of completely biological engineered grafts implanted into the sheep femoral artery. J Cardiovasc Transl Res. 2014; 7(2):242–9. [PubMed: 24429838]

[26]. Hoerstrup SP, Cummings Mrcs I, Lachat M, Schoen FJ, Jenni R, Leschka S, et al. Functional growth in tissue-engineered living, vascular grafts: Follow-up at 100 weeks in a large animal model. Circulation. 2006; 114(1 Suppl):I159–66. [PubMed: 16820566]

[27]. Brennan MP, Dardik A, Hibino N, Roh JD, Nelson GN, Papademitris X, et al. Tissue-engineered vascular grafts demonstrate evidence of growth and development when implanted in a juvenile animal model. Ann Surg. 2008; 248(3):370–7. [PubMed: 18791357]

[28]. Ivy DD, Abman SH, Barst RJ, Berger RM, Bonnet D, Fleming TR, et al. Pediatric pulmonary hypertension. J Am Coll Cardiol. 2013; 62(25 Suppl):D117–26. [PubMed: 24355636]

[29]. Rubin LJ. Primary pulmonary hypertension. N Engl J Med. 1997; 336(2):111–7. [PubMed: 8988890]

[30]. Fung, YC. Biomechanics: Mechanical properties of living tissues. 2 ed. Springer-Verlag; 1993.

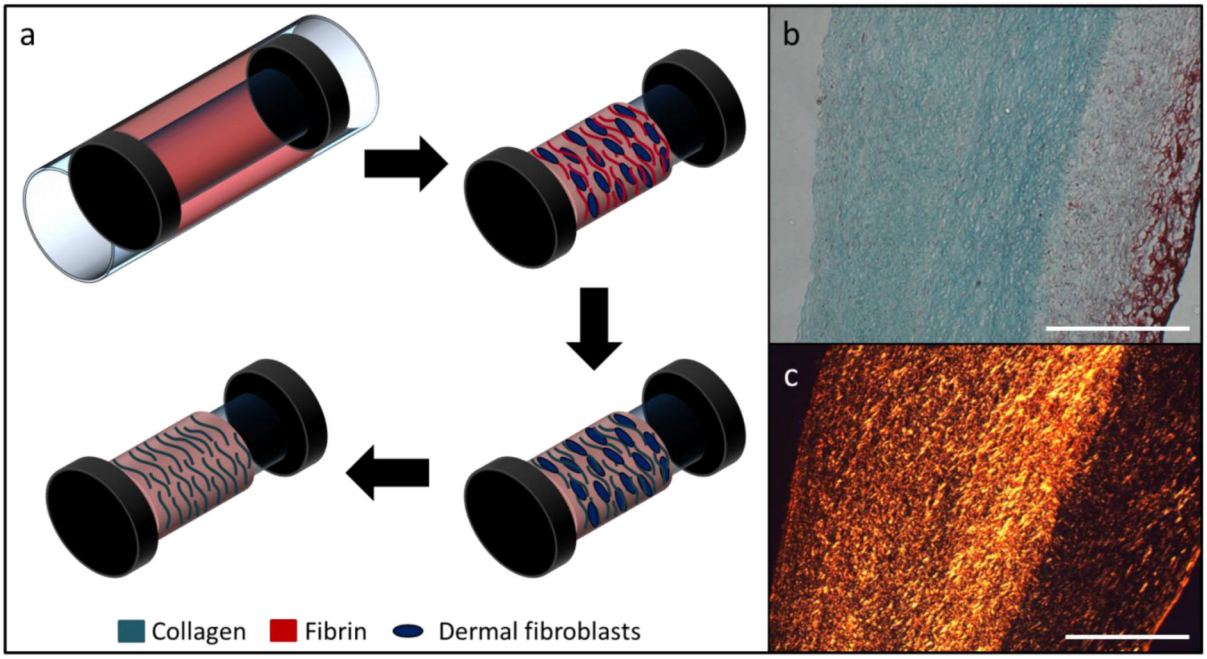

Figure 1.

(a) Tissue tube fabrication schematic. The entrapped dermal fibroblasts replace the initial fibrin gel with an aligned, collagenous matrix. The cell-produced matrix is left intact following decellularization. (b) Trichrome staining showing collagen (green) and non-collagen (fibrin, red) after decellularization. (c) Picrosirius red staining under crossed plane polarizers showing collagen fiber organization. Both scale bars are 500 μm.

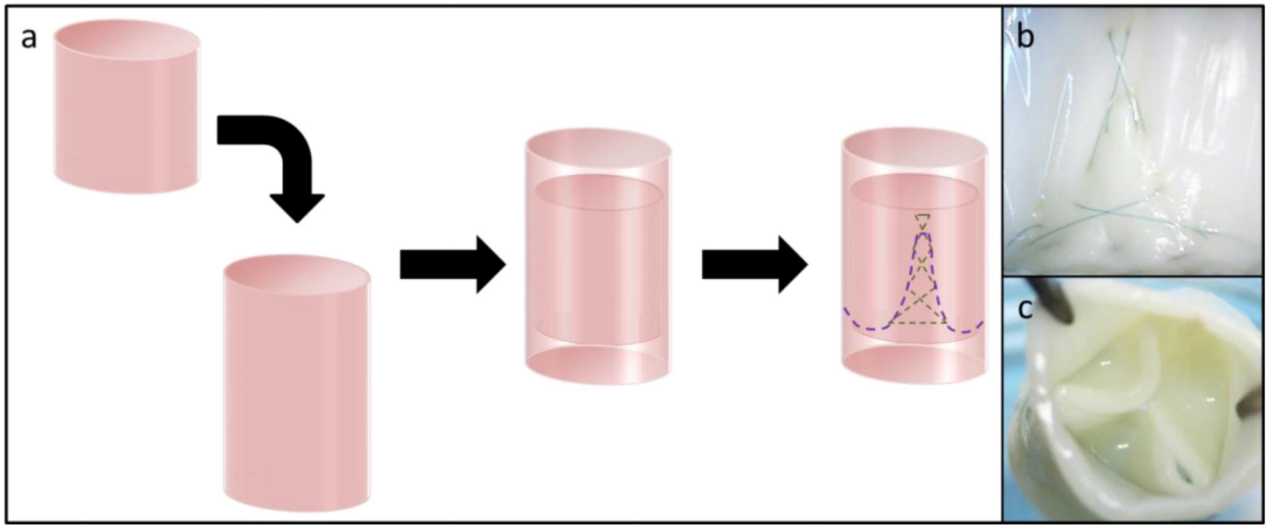

Figure 2.

(a) Schematic of a frameless tubular heart valve made from two concentric, engineered tissue tubes. They are attached using a degradable suture line (purple) that defines belly and commissure regions. (b) The commissure regions are reinforced with a secondary crosshatching pattern (see also green dashed line in (a)). (c) The inner tube collapses inward between the three commissures when the valve is exposed to back pressure, which generates three “leaflets” and a valve-like action.

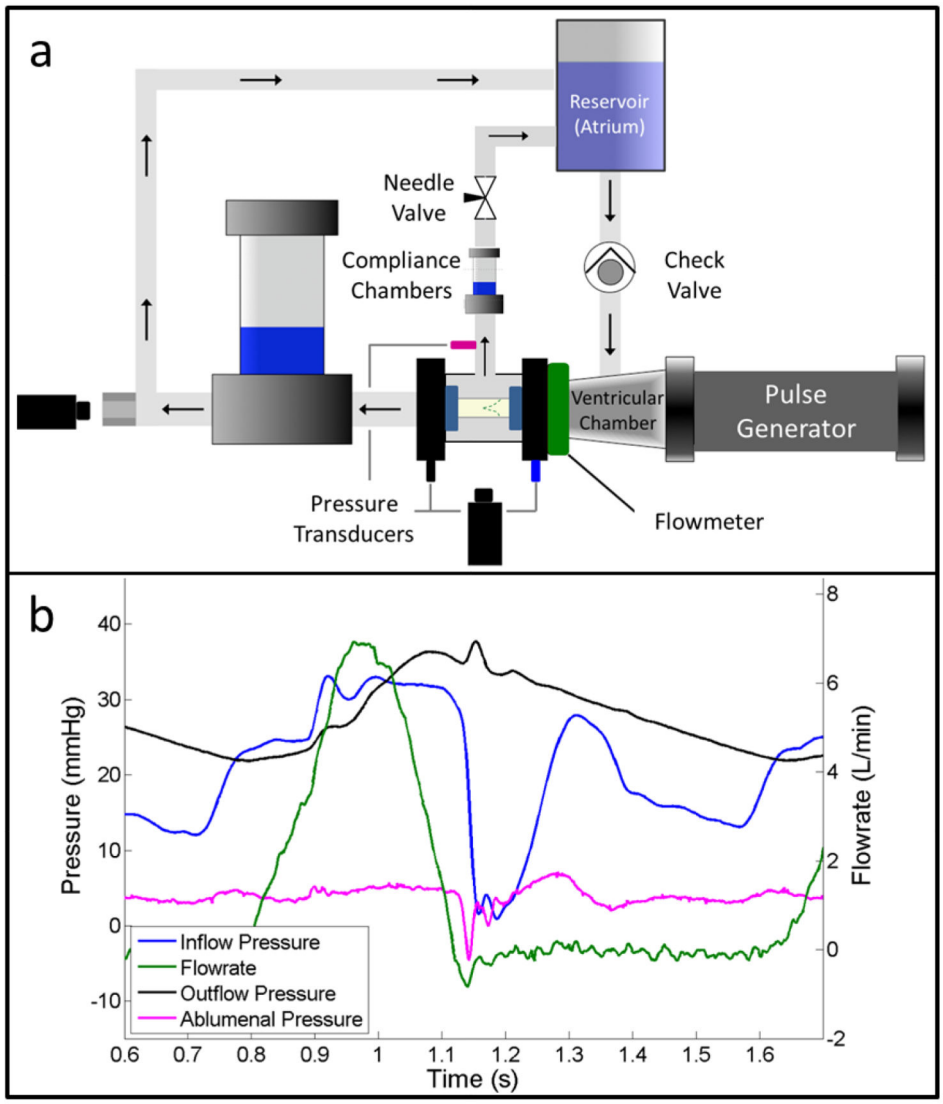

Figure 3.

The TEHVs were tested using (a) a custom pulse duplicator system, which allows valve root distention and trans-root flow. The valve test chamber is fluid-filled and is connected to the reservoir through a secondary flow loop. (b) A representative flow-pressure trace is shown under pulmonary conditions. The locations of pressure probes and corresponding pressure traces are color coded in the panels. A water hammer effect typical in pulse duplicator systems affects all of the pressure traces, but is most evident in the inflow pressure (at time=~1.15).

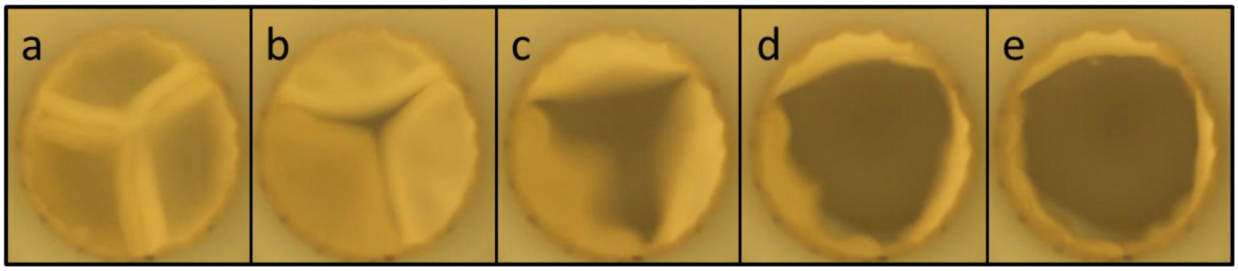

Figure 4.

Images of leaflet motion during valve testing in a pulse duplicator system under pulmonary flow conditions. (a) Leaflet coaptation is maintained during diastole, but (b-d) rapidly opens as systole begins. (e) Full valve opening is achieved before the leaflets begin to close.

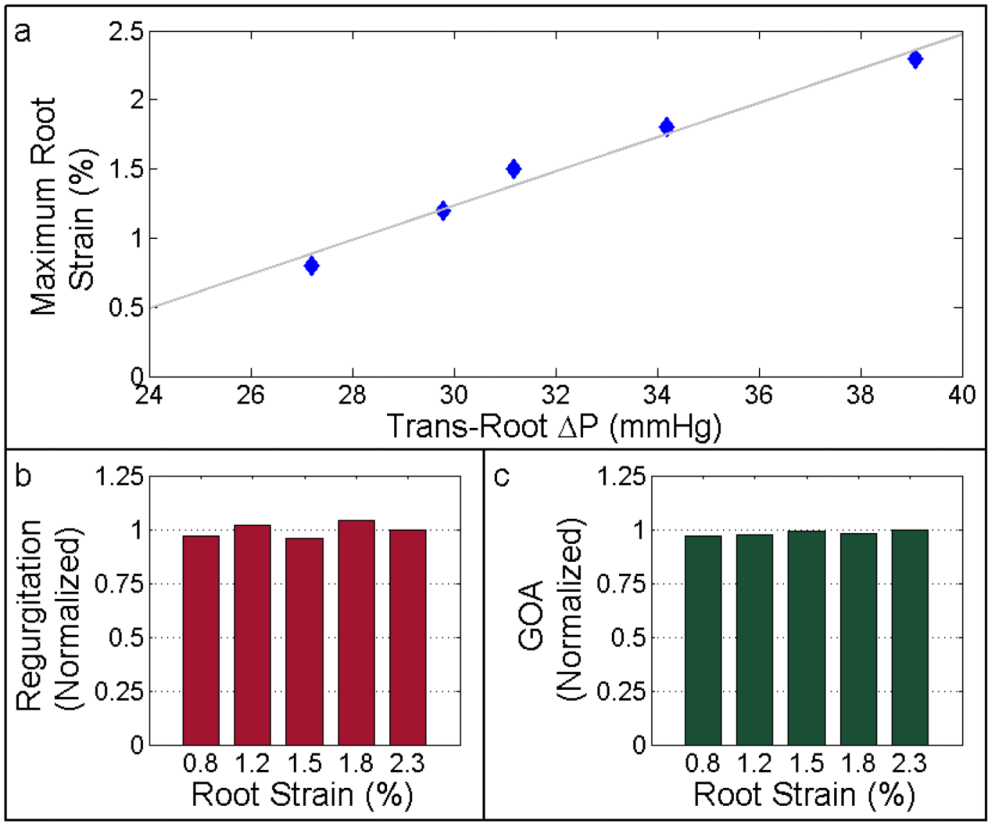

Figure 5.

Ablumenal pressure was manipulated to assess TEHV performance under various trans-root pressure gradients. (a) TEHV root strain shown as a function of the trans-root pressure gradient. TEHV (b) regurgitation and (c) geometric orifice area are normalized to their respective values using the maximum trans-root strain/pressure gradient case.

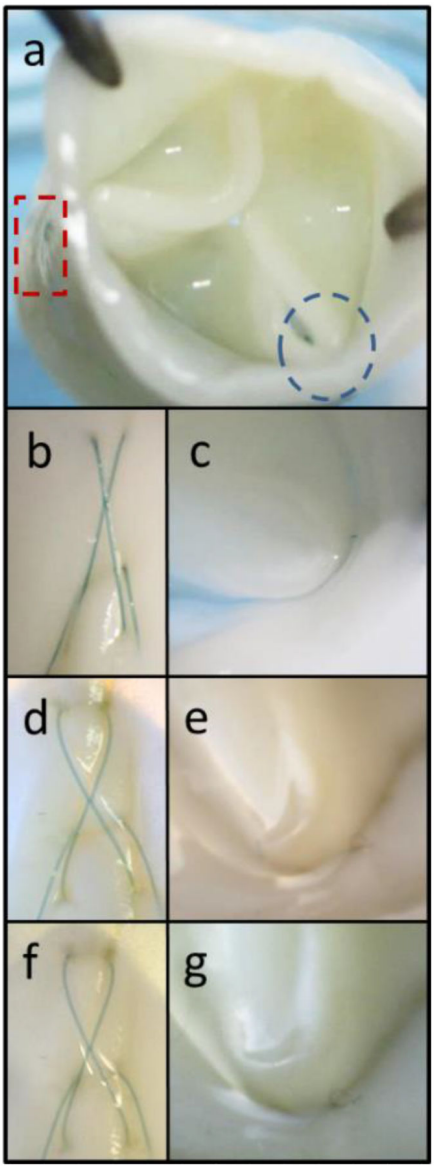

Figure 6.

Macroscopic images of a TEHV fatigued in the pulse duplicator system for 2 weeks at 100 cycles/minute. Images were taken near the commissures on the (a, rectangle) ablumenal or (a, circle) lumenal surface. The TEHV was macroscopically analyzed at the same locations (b-c) before fatiguing, (d-e) after 1 week, and (f-g) following completion of testing at 2 weeks.

Table 1

Mechanical Properties of a Commercial, Pulmonary Bioprosthetic Valve & the Engineered Tubes

Property	Contegra Valve	Engineered Tubes
Leaflet Thickness (*mm*)	0.21 ± 0.03	1.35 ± 0.05
Leaflet Circumferential UTS (*MPa*)	3.3 ± 1.1	1.5 ± 0.4
Leaflet Circumferential Modulus (*MPa*)	12.6 ± 1.8	5.2 ± 0.6
Leaflet Modulus Anisotropy	N/A	3.8 ± 0.9
Root Thickness (*mm*)	0.76 ± 0.10	1.35 ± 0.05
Root Circumferential UTS (*MPa*)	3.4 ± 0.3	1.5 ± 0.4
Root Circumferential Modulus (*MPa*)	6.5 ± 0.1	5.2 ± 0.6
Root Modulus Anisotropy	1.0 ± 0.1	3.8 ± 0.9

Table 2

Pulse Duplicator Testing of TEHVs Compared with a Commercial, Pulmonary Bioprosthetic Valve

Property	Contegra Valve	TEHVs (n=3)
Mean Diastolic ΔP (*mmHg*)	16.5	14.5 ± 3.7
Mean Systolic ΔP (*mmHg*)	3.3	2.4 ± 0.1
Mean Ablumenal Pressure (*mmHg*)	4.3	3.5 ± 0.7
Mean Forward Flow Rate (*L/min*)	3.4	3.6 ± 0.2
Regurgitant Fraction	7.3%	4.8% ± 0.8%
Geometric Orifice Area	52%	76% ± 15%

Table 3

Pulse Duplicator Testing Before, During, and After TEHV Fatiguing

Property	T = 0 weeks	T = 1 Week	T = 2 weeks
Mean Diastolic ΔP (*mmHg*)	13.2	11.9	11.4
Mean Systolic ΔP (*mmHg*)	2.5	1.8	3.1
Mean Ablumenal Pressure (*mmHg*)	4.0	3.0	1.4
Mean Forward Flow Rate (*L/min*)	3.6	3.2	3.8
Regurgitant Fraction	3.9%	12.9%	13.8%
Geometric Orifice Area	81%	89%	87%